PIP2-dependent regulation of Munc13-4 endocytic recycling: impact on the cytolytic secretory pathway

Cristina Capuano,[1] Rossella Paolini,[2] Rosa Molfetta,[2] Luigi Frati,[2,3] Angela Santoni,[2,3] and Ricciarda Galandrini[1]

Departments of [1]Experimental Medicine and [2]Molecular Medicine, Istituto Pasteur–Fondazione Cenci-Bolognetti, Fondazione Eleonora Lorillard Spencer Cenci, Sapienza University, Rome, Italy; and [3]Istituto Mediterraneo di Neuroscienze Neuromed, Pozzilli, Italy

Cytotoxic lymphocytes clear infected and transformed cells by releasing the content of lytic granules at cytolytic synapses, and the ability of cytolytic effectors to kill in an iterative manner has been documented previously. Although bidirectional trafficking of cytolytic machinery components along the endosomal pathway has begun to be elucidated, the molecular mechanisms coordinating granule retrieval remain completely unexplored. In the present study, we focus on the lytic granule priming factor Munc13-4, the mutation of which in familial hemophagocytic lymphohistiocytosis type 3 results in a profound defect of cytotoxic function. We addressed the role of phosphatidylinositol (4,5)-bisphosphate (PIP2) in the regulation of Munc13-4 compartmentalization. We observed that in human natural killer cells, PIP2 is highly enriched in membrane rafts. Granule secretion triggering induces a transient Munc13-4 raft recruitment, followed by AP-2/clathrin–dependent internalization. Phosphatidylinositol 4-phosphate 5-kinase (PIP5K) γ gene silencing leads to the impairment of granule secretion associated with increased levels of raft-associated Munc13-4, which is attributable to a defect in AP-2 membrane recruitment. In such conditions, the ability to subsequently kill multiple targets was significantly impaired. These observations indicate that Munc13-4 reinternalization is required for the maintenance of an intracellular pool that is functional to guarantee the serial killing potential. (*Blood*. 2012;119(10):2252-2262)

Introduction

Natural killer (NK) cells and cytotoxic T lymphocytes are major players in the defense against tumors and viral infections, mediating target cell killing through the polarized secretion of cytotoxic mediators such as perforin and granzymes stored in specialized secretory lysosomes termed lytic granules.[1] This process involves several steps, including the formation of a cytolytic synapse and the rapid reorientation of the microtubule-organizing center and lytic granules toward the target contact area, followed by granule docking, priming, and fusion at specialized secretory domains.[2] Emerging evidence has demonstrated that the clustering of GM1-enriched membrane domains, termed membrane rafts, provides a necessary platform where the integration of molecular signals directing cytolytic machinery activation can occur.[3] Soluble-N-ethylmaleimide-sensitive-factor accessory-protein receptor (SNARE) family members are the highly conserved master regulators of membrane fusion events.[4] Phenotypic consequences of the genetic defects affecting lytic granule trafficking to the cytolytic synapse allow the dissection of the discrete steps of the cytotoxic event controlled by individual SNARE or SNARE-related factors.[5] In familial hemophagocytic lymphohistiocytosis (FHL) type 3, for example, mutations of UNC13D causing loss of hMunc13-4 function impair exocytosis of cytotoxic granules that have docked at the cytolytic synapse.[5,6] Analysis of Munc13-4–deficient cells showed that this protein critically regulates a priming step, conferring to the cytotoxic granules a fusion-competent state. Moreover, recent evidence has highlighted an intriguing additional role for Munc13-4 in driving lytic granule maturation.[7]

NK cells are able to successively kill several target cells in a short time period. The iterative killing ability depends on the combination of 2 factors: (1) that, after target recognition, only a fraction of the granule pool is released and (2) at the same time, cytotoxic proteins are newly synthesized to refill the store of cytotoxic component.[8,9] Recently, the rapid endocytosis of granule membrane proteins exposed at the plasma membrane on degranulation, including lysosome-associated membrane protein-1 (LAMP-1, also known as CD107a), has been described.[10] However, the molecular mechanisms controlling the retrieval of cytolytic machinery components and whether endocytic traffic is functional to guaranteeing the full cytolytic potential are still unknown.

Although PIP2 represents less than 1% of plasma membrane phospholipids, it is responsible for a wide range of membrane-related phenomena, including vesicle trafficking, actin dynamics, and ion channel regulation.[11,12] We reported recently that PIP5Kα and PIP5Kγ isoforms are the enzymes mainly responsible for PIP2 synthesis in human NK cells; both of them synergistically control IP3/Ca^{2+} levels required for lytic granule exocytosis, with PIP5Kγ also involved in regulating a Ca^{2+}-independent step.[13] In the present study, we investigated whether PIP5K isoforms are involved in the regulation of SNARE factor compartmentalization and thus affect NK-cell cytolytic potential. We report herein that the PIP5Kγ-dependent PIP2 pool acts in the control of the endocytic traffic of cytolytic machinery components, in particular by regulating clathrin/AP-2–dependent Munc13-4 endocytosis, which functions to ensure the full cytolytic potential.

Submitted December 9, 2010; accepted January 13, 2012. Prepublished online as *Blood* First Edition paper, January 23, 2012; DOI 10.1182/blood-2010-12-324160.

The online version of this article contains a data supplement.

The publication costs of this article were defrayed in part by page charge payment. Therefore, and solely to indicate this fact, this article is hereby marked "advertisement" in accordance with 18 USC section 1734.

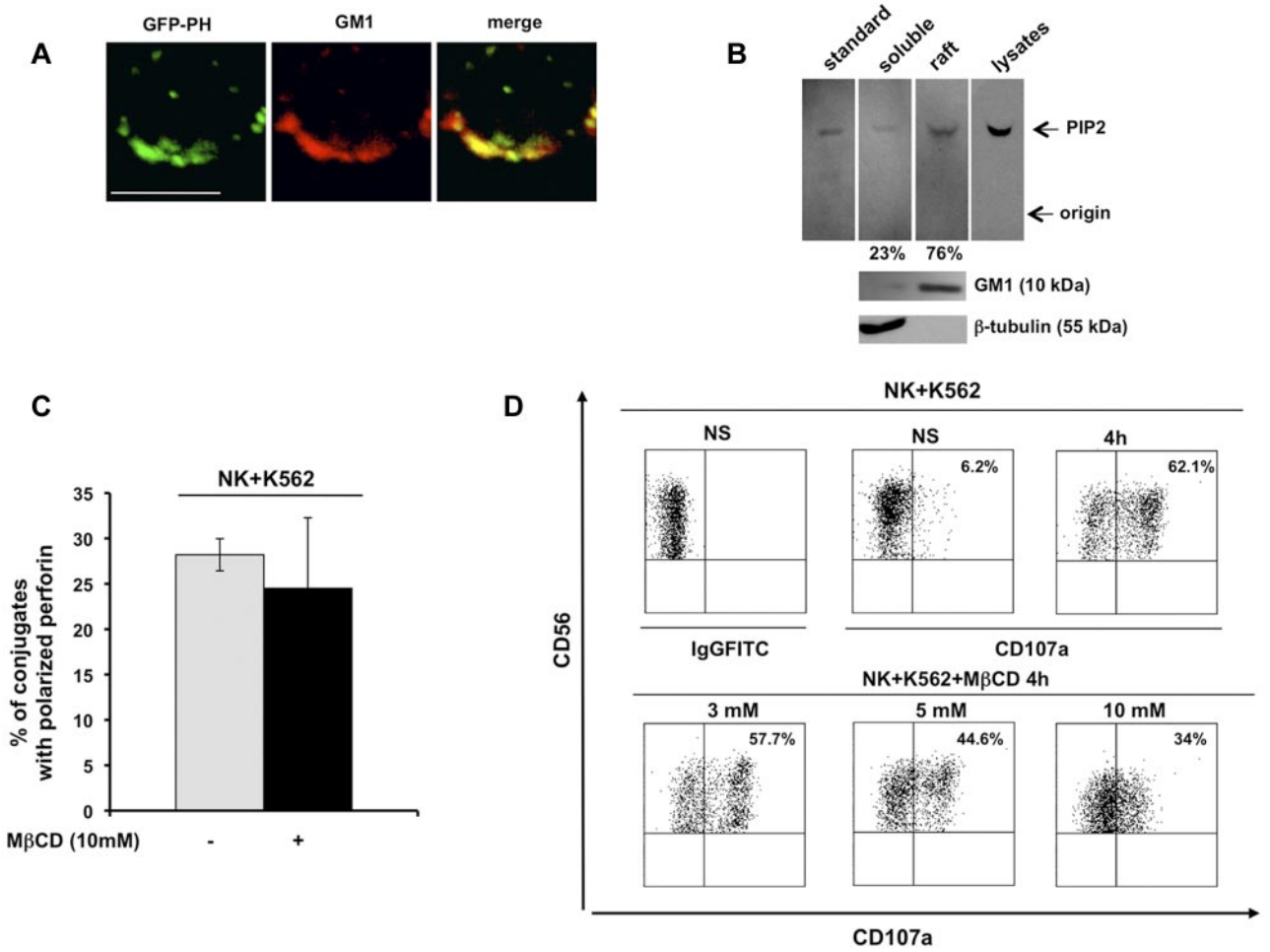

Figure 1. PIP2 colocalizes with membrane raft microdomains, the integrity of which is required for lytic granule exocytosis. (A) Primary cultured NK cells were infected with recombinant lentiviruses encoding GFP-PH fusion protein. Live cells were stained with Alexa Fluor 594–conjugated CTxB. GFP-PH and GM1 distribution was analyzed by confocal microscopy (left and middle panels), the colocalization of fluorescence signals is represented in right panel. Representative image from 3 independent experiments is shown. Bar represents 5 μm. (B) Total phospholipids were extracted from whole lysate or from raft and soluble fractions from primary cultured NK cells. Phosphoinositides were resolved by TLC, followed by immunoblotting with anti-PIP2 mAb (top panels). The spot corresponding to PIP2 in raft and soluble fractions was quantified by densitometric analysis; the numbers indicate the percentage of PIP2 distribution between raft and soluble fraction assuming the sum of PIP2 present in both compartments as 100%. One representative experiment of 3 performed is shown. GM1 and β-tubulin immunoblots of the same experiment are shown (bottom panels). (C) Primary cultured NK cells were left untreated or pretreated with MβCD and allowed to interact with a K562-sensitive target. Cell conjugates were fixed, stained with anti-perforin mAb, and analyzed by fluorescence microscopy. The percentage of NK/target cell conjugates containing polarized granules was calculated on randomly acquired fields of 3 independent experiments (means ± SD, n = 100 conjugates). The difference between the treated and untreated group was not significant. (D) Primary cultured NK cells were left untreated or pretreated with the indicated doses of MβCD and allowed to interact with K562 target cells (E:T ratio, 2:1). After 4 hours of stimulation, cells were stained with PE-conjugated anti-CD56 and the percentage of $CD107a^+$ cells was evaluated by cytofluorimetric analysis. Dot-plot analysis of gated $CD56^+$ cells is shown. One representative experiment of 3 performed is shown.

Methods

Abs and reagents

Anti-CD16 (B73.1) and anti–MHC class I (W6.32) mAbs were provided by Dr G. Trinchieri (National Cancer Institute, National Institutes of Health, Frederick, MD). Anti–DNAM-1 mAb (11A8) was kindly provided by Dr M. Colonna (Washington University School of Medicine, St Louis, MO). Anti-β2 integrin (TS1/18) mAb was provided by Dr F. Sanchez-Madrid (La Princesa Hospital, University of Madrid, Madrid, Spain). Anti-2B4 (CD244; C1.7) mAb was from Beckman Coulter. Anti–NKG2D (149810) mAb was from R&D Systems. Anti-PI5KIγ mAb was a kind gift from Dr P. De Camilli (Yale University School of Medicine, New Haven, CT). Anti–Munc13-4 Abs used for Western blot and fluorescence microscopic analysis were kindly provided by Dr H. Horiuchi (Kyoto University, Kyoto, Japan) and by Dr S. D. Catz (Scripps Research Institute, La Jolla, CA), respectively. Anti-syntaxin11 Ab was kindly provided by Dr R. Prekeris (Stanford University, Stanford, CA). Anti-EEA1 Ab was kindly provided by Dr M. Zerial (Max Planck Institute of Molecular Cell Biology and Genetics, Dresden, Germany). Anti–α-adaptin 1/2 (AP-2; C-8 and AP.6) and anti-Lck (3A5) mAbs, anti-PI5KIα (C-17) and anti-Rab7 (H-50) Abs, and normal mouse IgG were from Santa Cruz Biotechnology. Anti-syntaxin4, anti-Rab11, anti-CD45, PE- and FITC-conjugated anti-CD107a (H4A3), and PE-conjugated anti-CD56 mAbs were from BD Biosciences. The peroxidase-conjugated cholera toxin B (CTxB) subunit and anti–β-tubulin (Tub2.1) mAb and all chemicals were from Sigma-Aldrich. Anti-perforin mAb was from Ancell. Goat anti–mouse $F(ab')_2$ was from MP Biomedicals. Anti-PIP2 mAb was from Gene Tex. Anti-Vav mAb was from Upstate Biotechnology. Alexa Fluor 594–conjugated CTxB subunit and Alexa Fluor 350–conjugated goat anti–mouse and donkey anti–rabbit Abs were from Molecular Probes. Anti-CTxB subunit Ab and 1,2 bis(o-aminophenoxy)ethane-NNN′N′-tetraacetic acid (BAPTA/AM) were from Calbiochem.

Cell systems and lentiviral infection

The human EBV^+ lymphoblastoid cell lines 721.221, the erythroleukemia line K562, the FcR^+ mouse mastocytoma lines P815 and YTS, human NK cell line were maintained in RPMI 1640 medium supplemented with 10%

FCS and 1% L-glutamine. The human NK-cell line NK92 was cultured as described previously.[13] Primary cultured NK-cell populations were obtained as described previously.[14] NK cells were infected with the recombinant plasmid pWPT-GFP-PH or with shRNA-encoding DNA sequences targeting PIP5Kα, PIP5Kβ, and PIP5Kγ as described previously[13,15]

Cell microscopy

To detect PIP2 distribution in membrane raft microdomains, green fluorescent protein–Pleckstrin homology (GFP-PH)–expressing live NK cells were stained with Alexa Fluor 594–conjugated CTxB (40 μg/mL) for 40 minutes at 4°C and spun on microscope slides. Images were acquired at room temperature with a laser confocal inverted microscope (TSC-SP2; Leica) with Plan APO 40× numerical aperture 1.25 oil objective. Images were captured and processed using Leica Confocal LAS AF software; 4 optical sections were merged.

To evaluate granule polarization, primary cultured NK cells were pretreated with methyl-β-cyclodextrin (MβCD) at 37°C for 30 minutes, stimulated with K562-sensitive target cells (effector:target [E:T] ratio, 2:1) and processed as described previously.[13] Images were acquired at room temperature using an ApoTome Observer Z.1 microscope (Carl Zeiss) with 40×/0.75 Plan-Neofluar objective and an Axiocam MR (all from Carl Zeiss). AxioVision Version 4.6.3 software (Carl Zeiss) was used for both acquisition and image processing. The ApoTome Zeiss system provides an optical slice view reconstructed from fluorescent samples using a series of "grid projection" acquisitions, as described previously[16] Imaging stacks in the axial direction were acquired and all images shown are from a representative axial plane. Granule polarization was assessed in NK/K562-cell conjugates showing an extensive membrane contact between effector and target cells and expressed as percentage of conjugates containing polarized granules with respect to total conjugates. P815 target cells, kept as a negative control, did not induce detectable granule polarization (C.C., unpublished data, October 10, 2009).

To evaluate Munc13-4 distribution in membrane rafts, YTS cells were labeled with Alexa Fluor 594–conjugated CTxB (20 μg/mL) for 1 hour at 4°C, and aggregated for 3 minutes at 37°C. Labeled cells were seeded onto poly-L-lysine–coated glass slides, fixed, and stained with anti–Munc13-4 Ab diluted 1:500 in PBS, 1% BSA, and 0.01% saponin, and incubated at 4°C overnight, followed by the addition of Alexa Fluor 350–conjugated secondary Ab. Images were acquired at a fluorescence excitation of 358 nm and an emission of 463 nm, visualized using a green dye, and shown as a representative axial plane. Colocalization of the fluorescence signal was analyzed with AxioVision Version 4.6.3 software (Carl Zeiss). Images were processed with Photoshop Version 7 software (Adobe).

Degranulation and cytotoxic assay

To determine CD107a surface expression,[17] NK cells were mixed with the sensitive target cells K562 (E:T ratio, 2:1) for 4 hours at 37°C in the presence of FITC-conjugated anti-CD107a or anti-IgG mAbs; 50μM monensin (GolgiStop; BD Biosciences) was added after the first hour. Cells were then stained with PE-conjugated anti-CD56 mAb, fixed with 2% paraformaldehyde, and analyzed by flow cytometry. When indicated, cells were pretreated (30 minutes) with MβCD. YTS cells were stimulated by the addition of phorbol-12-myristate-13-acetate (PMA) and ionomycin (see next paragraph) for 4 hours at 37°C. After 1 hour of stimulation, 3mM monensin was added.

Primary cultured YTS and NK92 NK cells were assessed in a ^{51}Cr-release assay.[14] Where indicated, NK cells were pretreated with BAPTA/AM for 30 minutes at 37°C and tested in a redirected killing ^{51}Cr-release assay against P815 cells in the presence of anti-CD16 mAb. Cycloheximide (50 μg/mL) was added during the ^{51}Cr-release assay. Killing frequency was evaluated by dividing the number of killed targets by the number of effector cells for each E:T ratio.[8]

Raft isolation and subcellular fractionation

Membrane rafts were isolated from primary cultured NK cells (200×10^6 cells/sample) or YTS cells (90×10^6 cells/sample) as described previously.[14] When required, primary cultured NK cells were pretreated (30 minutes) and then stimulated in the presence of 20μM BAPTA/AM. For clathrin-coated pit disruption, cells were subjected to hypotonic shock by rinsing with K^+-free buffer (140mM NaCl, 20mM HEPES, 1mM $CaCl_2$, 1mM $MgCl_2$, and 1 mg/mL of D-glucose, pH 7.4) and then incubated for 5 minutes at 37°C with hypotonic buffer (RPMI 1640 medium supplemented with 10% FCS and 1% L-glutamine diluted 1:1 with distilled water). Cells were then stimulated in K^+-free buffer. For dynamin blocking, primary cultured NK cells were stimulated in the presence of 80μM Dynasore (Sigma-Aldrich). Membrane and cytosolic fractions were obtained as described previously.[18]

Cell stimulation and immunoprecipitation

For mAb-mediated receptor cross-linking, NK cells were incubated for 15 minutes at 4°C with a saturating dose of anti-CD16, anti-2B4, anti-NKG2D, anti–DNAM-1, and anti-β2 mAbs (all mouse IgG1 isotype), alone or in combination where indicated, followed by goat anti–mouse $F(ab')_2$ at 37°C. The control group was incubated with isotype-matched mAbs for 10 minutes at 37°C. Alternatively, NK or YTS cells were stimulated with ionomycin (0.5 μg/mL) plus PMA (50 ng/mL or 3 μg/mL, respectively), and the control group was incubated with vehicle-containing medium.

To analyze the Munc13-4 and AP-2 interaction, YTS cells were lysed in 50mM Tris, pH 7.5, 150mM NaCl, 1mM EGTA, pH 8, 1mM $MgCl_2$, 50mM NaF, and 1% N-octylglucoside and immunoprecipitated with α-adaptin 1/2 (AP.6 or C-8) mAb.

Phosphoinositide analysis

To analyze PIP2 distribution in membrane rafts, low-density (1-6) and high-density (7-12) fractions isolated from primary cultured NK cells were pooled and phosphoinositide extraction was performed as described previously.[13] For immunoblot analysis, thin-layer chromatography (TLC) plates were treated with 0.5% methacrylate and revealed with anti-PIP2 mAb.

Statistical and densitometric analysis

All results were analyzed with the 2-tailed *t* test. Values are expressed as means ± SD and differences were considered to be statistically significant at $P < .05$. Densitometric analysis was performed with ImageJ Version 64 software.

Results

PIP2 compartmentalization in membrane raft microdomains

The chimeric construct GFP-PH, which is known to bind PIP2 with high affinity and specificity, is a useful tool with which to investigate endogenous PIP2 distribution and functions.[19] In the present study, we examined PIP2 distribution in detergent-insoluble, GM1-enriched membrane domains. Primary cultured human NK cells infected with recombinant lentivirus encoding the GFP-PH fusion protein were stained with Alexa Fluor 594–conjugated CTxB, which identifies membrane ganglioside GM1. Confocal microscopic analysis revealed a strong colocalization signal of the GFP-PH construct with GM1 in unfixed cells (Figure 1A).

PIP2 membrane raft compartmentalization was also validated by TLC analysis of phospholipids extracted from raft and soluble compartments on sucrose gradient ultracentrifugation. Phosphoinositides extracted from low- and high-density fractions (see next paragraph) were resolved by TLC and revealed by immunoblot analysis. In agreement with the confocal microscopic data, raft fractions exhibited a considerable PIP2 enrichment (Figure 1B) with respect to soluble fraction. These findings indicate that PIP2 is highly enriched in membrane rafts.

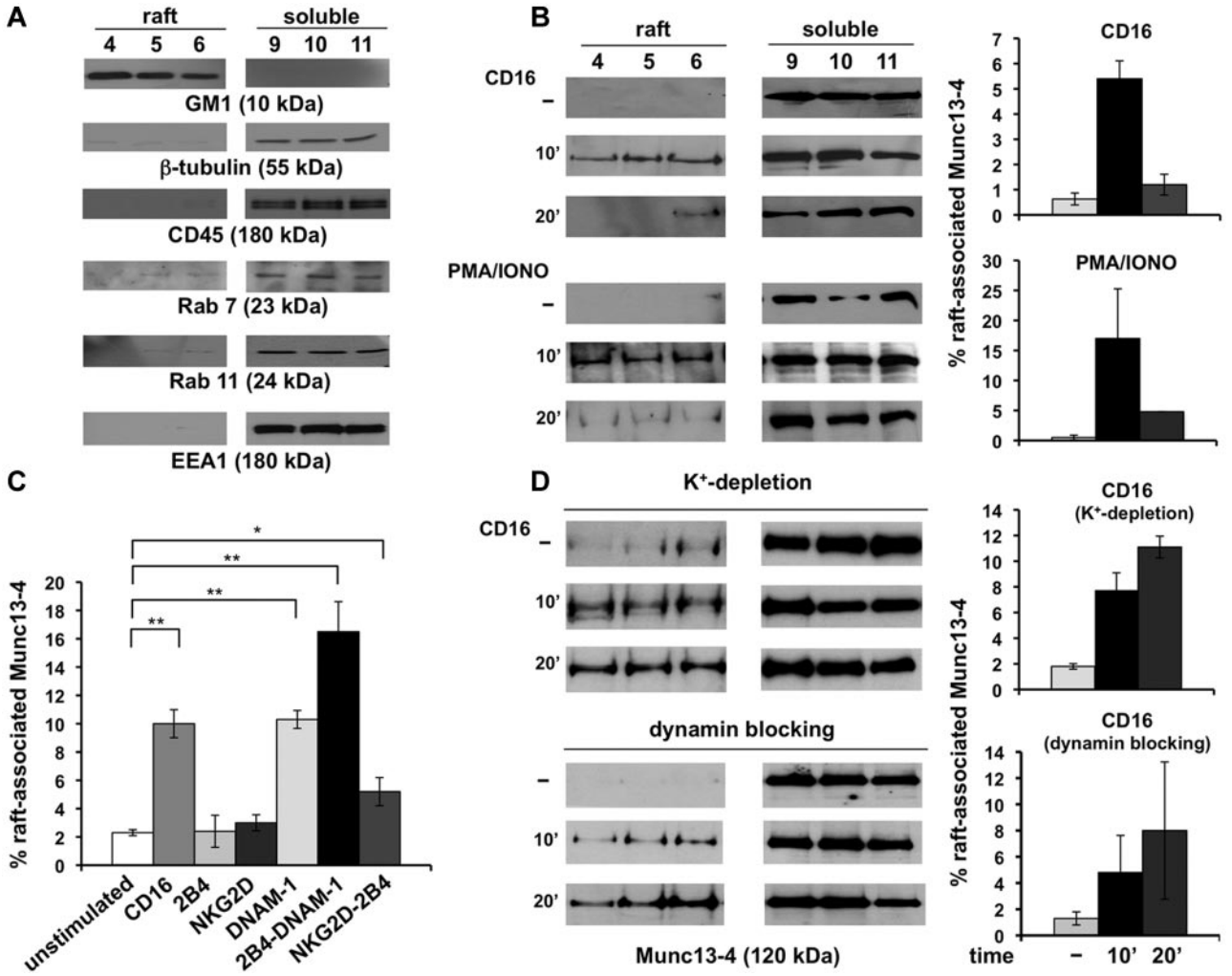

Figure 2. Munc13-4 is transiently recruited in membrane rafts after NK-cell activation. Primary NK cells were fractionated by sucrose gradient centrifugation. An equal amount of proteins recovered from the raft and detergent-soluble fractions were analyzed by Western blot. Unstimulated samples (−) were treated as described in "Methods." (A) The purity control of the raft and soluble fractions was performed by immunoblotting as indicated. One representative experiment is shown. (B) Cells were stimulated with anti-CD16 mAb or treated with PMA/ionomycin for the indicated times. Immunoblot analysis of raft and soluble fractions was performed. The percentage of raft-associated Munc13-4 was obtained by densitometric analysis evaluating the ratio of raft-associated Munc13-4 with respect to the total amount of Munc13-4 extrapolated by the sum of Munc13-4 levels in the single fractions normalized for the loaded volume (means ± SD, n = 3). (C) Cells were stimulated for 10 minutes with the indicated mAbs. The percentage of raft-associated Munc13-4 was evaluated as in panel B (means ± SD, n = 5). Differences between unstimulated and CD16-, DNAM-1-, 2B4/DNAM-1-, and 2B4/NKG2D-stimulated cells were significant (*$P < .05$; **$P < .01$). (D) In the same experiment described in panel B, cells were subjected to hypotonic shock for K^+ depletion or treated with Dynasore and CD16 stimulation was performed as above. One representative experiment of 3 performed is shown. The percentage of raft-associated Munc13-4 was evaluated as above (means ± SD, n = 3).

Raft coalescence at cytolytic synapse has been shown to be critical for cytolytic machinery activation in NK cells.[3] To understand whether a selected step of the cytolytic pathway depends on raft integrity, we pretreated primary cultured NK cells with the cholesterol-depleting agent MβCD, and examined granule polarization and exocytosis after interaction with K562-sensitive target cells. Microscopic analysis of perforin distribution within effector/target conjugates showed that the ability to polarize lytic granules was unaffected in MβCD-treated cells with respect to control cells (Figure 1C). Conversely, at the same MβCD dose, the secretory step was significantly impaired, as evaluated by cytofluorimetric analysis of CD107a surface levels[17]: after K562 stimulation, the percentage of CD107a-positive NK cells was reduced by almost 50% compared with the control population (Figure 1D).

Our findings demonstrate that raft integrity is required for optimal lytic granule release, but is dispensable for granule polarization.

Munc13-4 undergoes transient activation-dependent membrane raft recruitment

We also analyzed membrane raft distribution of different SNARE family members. Primary cultured NK cells were fractionated by sucrose gradient ultracentrifugation into 12 fractions.[14] Lipid raft-containing fractions were marked by the exclusive presence of GM1, and cytosolic and nonraft membrane fractions were revealed by the exclusive presence of β-tubulin and CD45 in immunoblot analysis: fractions 4-6 and 9-11 are representative of the raft and soluble compartments, respectively (Figure 2A). We also ruled out a significant raft contamination with endosome-associated proteins by immunoblotting with late, recycling, and early endosomal markers such as Rab7, Rab11, and EEA1, respectively (Figure 2A).

We also investigated the distribution of syntaxin4, syntaxin11, and Munc13-4, and found that both syntaxin isoforms were constitutively enriched in raft fractions and their levels were not

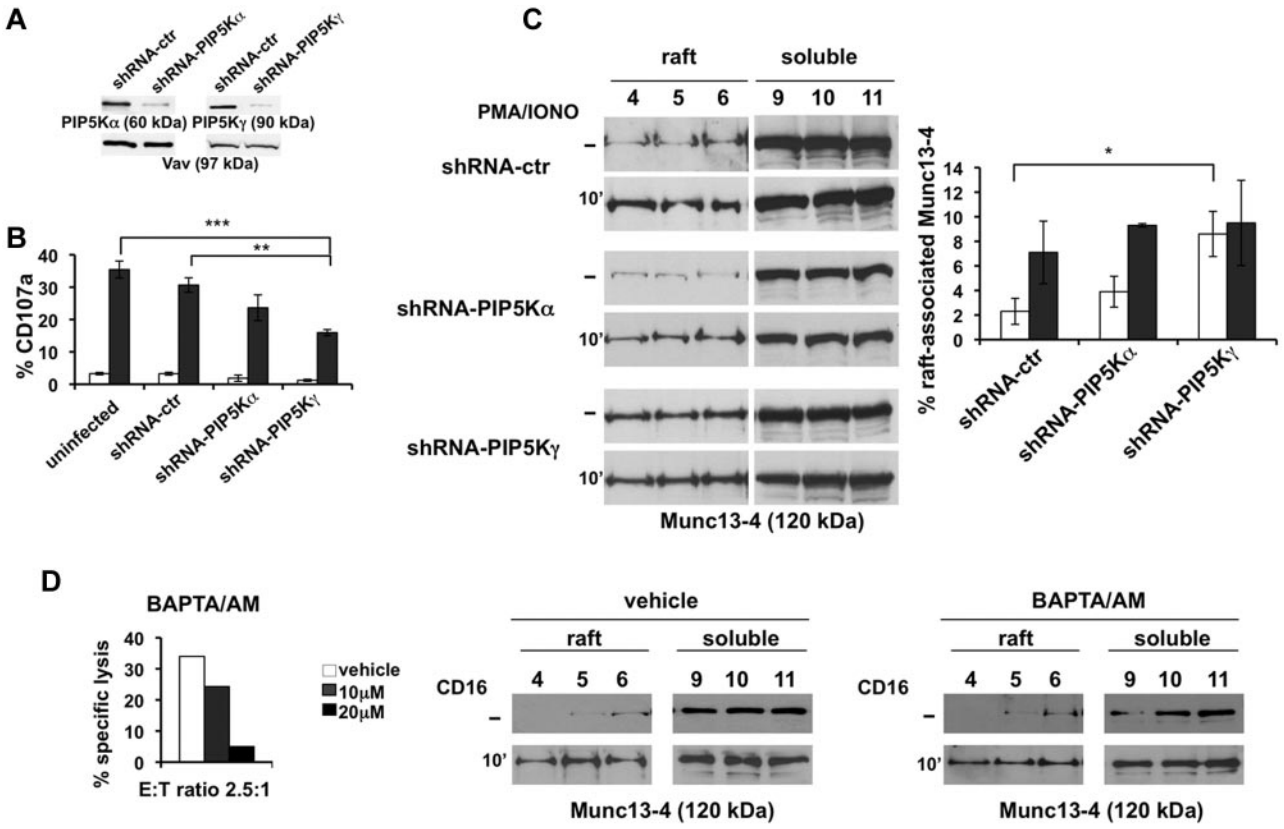

Figure 3. PIP5Kγ controls Munc13-4 membrane raft compartmentalization. (A) YTS cells were infected with lentiviruses encoding shRNA sequences targeting PIP5Kβ (shRNA-ctr), PIP5Kα (shRNA-PIP5Kα), or PIP5Kγ (shRNA-PIP5Kγ). Total cell lysates of infected populations were analyzed by immunoblotting with the indicated Abs. The same membrane was reprobed with anti-Vav mAb as loading control. (B) Uninfected, shRNA-ctr, shRNA-PIP5Kα–infected, and shRNA-PIP5Kγ–infected cells were tested in a degranulation assay. After 4 hours of PMA/ionomycin treatment (gray column), the percentage of $CD107a^+$ cells was evaluated by cytofluorimetric analysis. Unstimulated samples (white column) were treated as described in the "Cell stimulation and immunoprecipitation." Data represent the percentage (means ± SD) from 3 independent experiments. Differences between uninfected or shRNA-ctr and shRNA-PIP5Kγ-silenced cells were significant (**$P < .01$; ***$P < .005$). (C) shRNA-ctr, shRNA-PIP5Kα-, and shRNA-PIP5Kγ–silenced cells were treated with PMA/ionomycin. Unstimulated samples (−) were treated as described in "Methods." Raft and soluble compartments were isolated and equal amount of proteins were analyzed by immunoblotting with anti–Munc13-4 Ab. One representative experiment of 3 performed is shown. Percentage of raft-associated Munc13-4 in unstimulated (white column) and PMA/ionomycin–treated cells (gray column) was obtained by densitometric analysis (right panel) as described in Figure 2B. The difference (*$P = .05$) between unstimulated shRNA-ctr and shRNA-PIP5Kγ populations was significant. Data from 3 independent experiments (means ± SD) are shown (right panel). (D) Primary cultured NK cells were tested in a CD16-induced redirected killing assay toward P815 target cells in the presence of the indicated amounts of BAPTA/AM (left panel). NK cells were pretreated with BAPTA/AM (20μM) or control medium (vehicle) and left unstimulated (−) or stimulated with anti-CD16. Distribution of Munc13-4 in raft and soluble fractions was analyzed by immunoblotting (middle and right panels). One representative experiment of 3 performed is shown.

modulated after CD16 stimulation (supplemental Figure 1, available on the *Blood* Web site; see the Supplemental Materials link at the top of the online article). In contrast, Munc13-4 was barely detected in the raft fractions of unstimulated cells (Figure 2B); interestingly, the induction of granule secretion by CD16 ligation or PMA/ionomycin treatment induced a transient Munc13-4 raft recruitment that was maximal at 10 minutes and reduced to almost basal levels within 20 minutes of stimulation. Quantitative analysis revealed that a fraction of Munc13-4 ranging from 5%-24% had undergone membrane raft association (Figure 2B). Natural cytotoxicity involves signal integration from different activating receptors, so the next step was to investigate whether their engagement, alone or in combination, could regulate Munc13-4 raft mobilization. Our findings showed that, differently from NKG2D and 2B4, DNAM-1 individual engagement was able to induce a significant Munc13-4 raft recruitment that was up-regulated under conditions of DNAM-1 and 2B4 coengagement. Further, only the simultaneous aggregation of NKG2D and 2B4 was able to promote Munc13-4 mobilization (Figure 2C).

To investigate whether raft-associated Munc13-4 could undergo reinternalization, we perturbed the endocytic route by removing clathrin lattices from membrane by potassium depletion or by treatment with the dynamin inhibitor Dynasore.[20,21] Our experiments showed that, under these conditions, Munc13-4 was retained in raft fractions at later points of CD16 stimulation (Figure 2D) or PMA/ionomycin treatment (C.C., unpublished data, June 25, 2009).

These results show that endogenous Munc13-4 transiently translocates to membrane rafts during the activation of secretory pathway and indicate that it undergoes reinternalization via a clathrin-dependent process.

PIP5Kγ silencing affects Munc13-4 compartmentalization

Our previous study demonstrated that the ubiquitous PIP5Kα and the neuronal PIP5Kγ isoforms represent the major PIP2-synthesizing enzymes in NK cells.[13]

PIP5Kα and PIP5Kγ were individually knocked down by lentiviral vector-driven shRNA. Because of the low transduction efficiency of primary NK cells that precludes genetic manipulation-based studies, in this set of experiments, we used the YTS cell line, a useful model for the study of NK-cell biology.[22] NK cells were infected with PIP5Kα- and PIP5Kγ-specific shRNA-encoding sequences, keeping the PIP5Kβ sequence as a negative control.

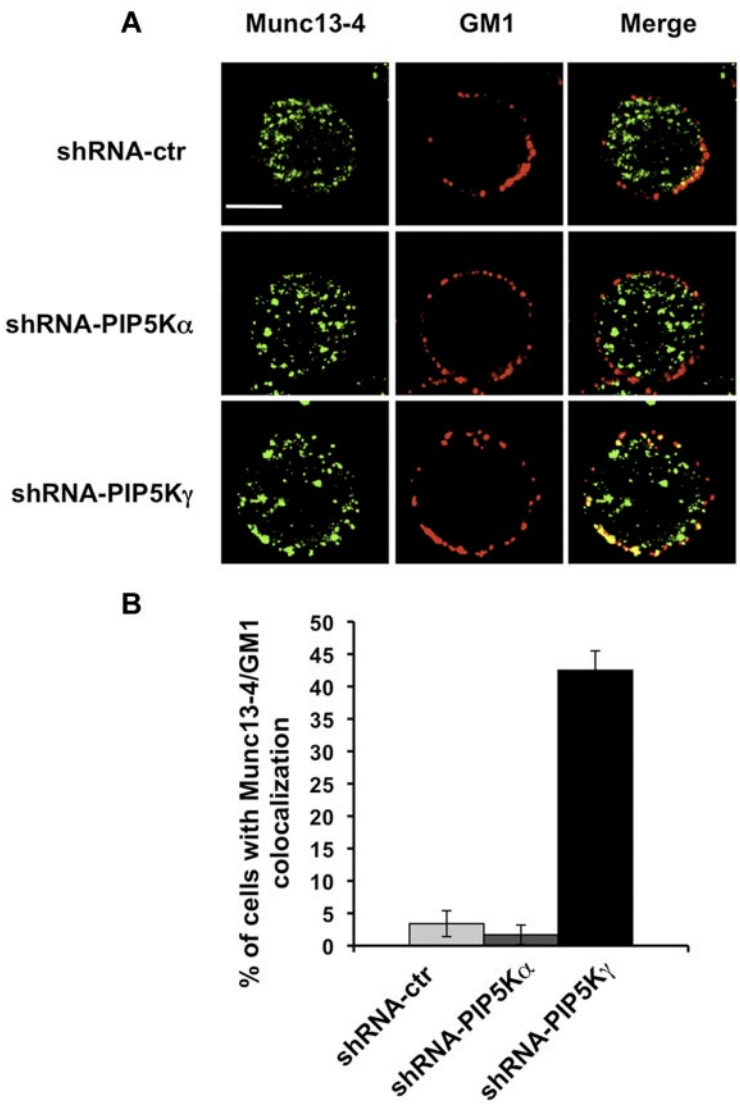

Figure 4. Munc13-4/GM1 colocalization in PIP5Kγ-silenced cells. (A) shRNA-ctr, shRNA-PIP5Kα, and shRNA-PIP5Kγ YTS cells were labeled with Alexa Fluor 594–conjugated CTxB. After fixing and permeabilization, samples were stained with anti–Munc13-4 Ab, followed by Alexa Fluor 350–conjugated secondary Ab. Fluorescent microscopic analysis using the ApoTome system was performed, and representative images of isolated cells are shown as a single optical section. Colocalization of fluorescence signals was analyzed with AxioVision Version 4.6.3 software. Bar represents 10 μm. (B) Percentage of cells showing Munc13-4 and GM1 colocalization was analyzed on randomly acquired fields (n = 80 cells) of each population. Data from 3 independent experiments (means ± SD) are shown.

The effects of the specific shRNAs on the steady-state levels of endogenous PIP5Kα and PIP5Kγ were analyzed (Figure 3A).

In agreement with our previous data,[13] we observed that the knock-down of PIP5K enzymes differently affects the secretory step. When NK cells were stimulated with PMA/ionomycin, surface CD107a levels were significantly lower in PIP5Kγ-silenced cells (almost 50%) and, to a lesser extent, in PIP5Kα-silenced cells (almost 30%) with respect to control populations, indicating that the PIP5Kγ-dependent PIP2 pool regulates granule exocytosis in a Ca^{2+}-independent manner (Figure 3B).

To investigate the contribution of the distinct PIP5K isoforms in the regulation of Munc13-4 membrane raft compartmentalization, we analyzed the distribution of endogenous Munc13-4 on secretory pathway activation under maximal stimulation conditions reached with PMA/ionomycin treatment. As shown in Figure 3C (top and middle panels), we observe that in PIP5Kα-silenced cells, Munc13-4 raft distribution is superimposable to that observed in control virus–infected cells, both in basal and activated conditions. Surprisingly, in PIP5Kγ-silenced cells, we observed a significant increase of Munc13-4 levels in membrane rafts under basal conditions that were not modulated by PMA/ionomycin stimulation (Figure 3C bottom panels).

We also wanted to address whether the PIP5Kγ-dependent PIP2 pool would control Munc13-4 dynamics downstream of receptor engagement. As observed in primary NK cells (Figure 2C), DNAM-1 is unique among other activating receptors (ie, 2B4, LFA-1 β2 integrin, and NKp46; C.C., unpublished data, October 15, 2011) in its ability to promote Munc13-4 raft recruitment in YTS cells (supplemental Figure 2). Further, as observed in CD16-stimulated primary cells (Figure 2B top panels), DNAM-1–induced Munc13-4 mobilization was transient, being reduced to almost basal levels within 20 minutes of stimulation. In the absence of PIP5Kγ, Munc13-4, which is constitutively present in membrane raft, is retained in such a fraction until the later time points of stimulation (supplemental Figure 2), suggesting that receptor-activated PIP5Kγ acts in the control of Munc13-4 reinternalization.

To investigate whether Munc13-4 mislocation could be related to the reduced IP3/Ca^{2+} levels that we described previously in PIP5K-silenced cells,[13] we analyzed Munc13-4 raft recruitment in the presence of the membrane-permeant Ca^{2+} chelator BAPTA/AM. At a BAPTA/AM concentration inducing a complete block of CD16-dependent cytotoxic function (Figure 3D left panel), we observed that CD16 stimulation induced Munc13-4 raft recruitment at an extent similar to that of the untreated population (Figure

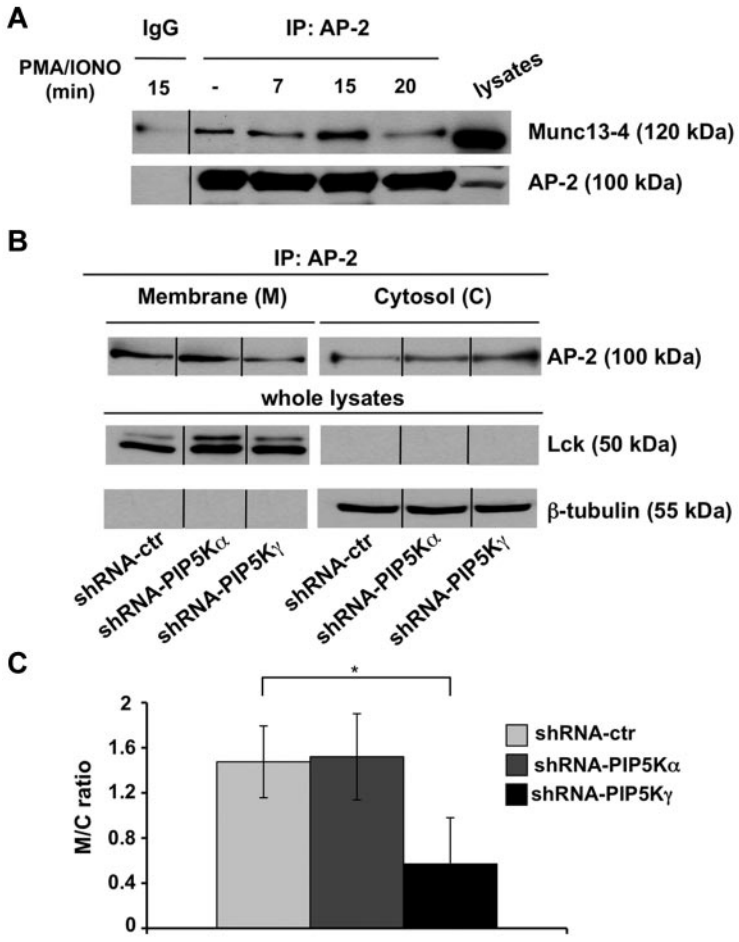

Figure 5. PIP5Kγ silencing reduces AP-2 membrane–bound levels. (A) YTS cells were treated with PMA/ionomycin for the indicated times. Cell lysates were precipitated with normal mouse IgG or α-adaptin1/2 (AP-2) mAb and AP-2/Munc13-4 complexes formation was evaluated by immunoblot analysis as indicated (top panel). The same membrane was reprobed with anti–α-adaptin mAb as a oading control (bottom panel). One representative experiment of 3 performed is shown. (B) AP-2 immunoprecipitates were obtained from membrane and cytosolic fractions isolated from shRNA-ctr, shRNA-PIP5Kα, and shRNA-PIP5Kγ YTS cell populations and analyzed by immunoblot (top panel). Total lysates of the same samples were analyzed by immunoblotting with the indicated mAbs as purity and loading controls (middle and bottom panels). One representative experiment of 3 performed is shown. (C) Quantitative analysis of the ratio of AP-2 levels in the membrane and cytosolic fractions shows a significant difference (*$P < .05$) between shRNA-ctr and shRNA-PIP5Kγ populations. Means from 3 independent experiments ± SD are graphed.

3D middle and right panels). These data further indicate that PIP5Kγ acts in a Ca^{2+}-independent manner in the control of Munc13-4 raft trafficking.

We then examined by fluorescence microscopy the distribution of endogenous Munc13-4. NK cells were stained with Alexa Fluor 594–conjugated CTxB and, after fixing and permeabilization, stained with anti-Munc13-4 Ab. In agreement with previous results showing Munc13-4 associating with recycling endosomes,[7] we observed a vesicular distribution pattern in our NK-cell populations (Figure 4A). When we analyzed the percentage of cells exhibiting Munc13-4/raft colocalization, we observed in PIP5Kγ-silenced cells, but not in PIP5Kα-silenced cells, that a portion of Munc13-4 colocalized (bottom panels) with membrane rafts in almost 50% of the cells (Figure 4B).

These findings indicate that the lack of the PIP5Kγ-dependent PIP2 pool is responsible for retention of the Munc13-4 membrane raft.

PIP5Kγ-dependent PIP2 pool controls Munc13-4 endocytic pathway

We investigated whether the Munc13-4 raft retention observed in PIP5Kγ-deficient cells could be because of its defective endocytosis. We first analyzed whether Munc13-4 associates with endogenous AP-2 clathrin adaptor, and our data showed that in basal conditions, a fraction of AP-2 coprecipitates with Munc13-4. Such an association transiently increases after PMA/ionomycin treatment, being maximal at 15 minutes and reduced to almost basal levels within 20 minutes of stimulation (Figure 5A).

Because AP-2 function strictly depends on its plasma membrane localization, we investigated whether PIP5Kγ regulates AP-2 compartmentalization at the plasma membrane. Endogenous AP-2 was immunoprecipitated from cytosolic and membrane compartments and the distribution of AP-2 was evaluated by Western blot analysis. We observed that AP-2 was constitutively enriched at the plasma membrane in both PIP5Kα-silenced and control virus–infected cells compared with the cytosolic fraction. Conversely, we detected a significant shift of AP-2 toward the cytosolic fraction with a consequent decreased amount of membrane-bound levels in PIP5Kγ-silenced cells (Figure 5B). The membrane/cytosol ratio showed a significant defect of membrane-bound AP-2 levels in PIP5Kγ-silenced cells (Figure 5C).

These findings suggest that the PIP5Kγ-dependent PIP2 pool controls Munc13-4 endocytosis by regulating AP-2 plasma membrane levels.

PIP5Kγ-dependent PIP2 pool controls the ability to serially mediate cytotoxic events

Our observed reinternalization of Munc13-4, along with the recent finding of the retrieval of CD107a-associated membranes after lytic granule exocytosis,[10] led us to the hypothesis that bidirectional trafficking at the cytolytic synapse could facilitate recycling and reuse of cytolytic machinery components by cytotoxic cells. To confirm this, we investigated whether the impairment of the Munc13-4–recycling pathway in PIP5Kγ-deficient cells could be correlated with a reduced ability to execute multiple killing cycles.

To estimate how many target cells are actually killed by an individual effector cell, we performed a 4-hour and an 8-hour ^{51}Cr-release assay at very low E:T ratios.[8] The killing frequency expresses the amount of target cells lysed per individual NK cell,

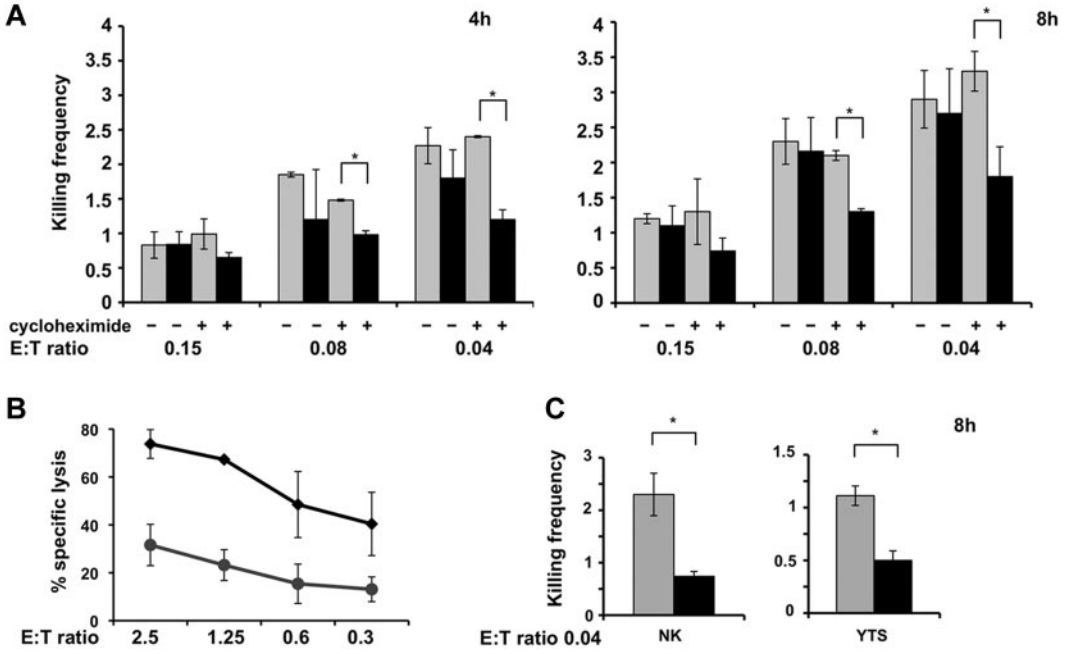

Figure 6. PIP5Kγ-silenced cells exhibit an impaired killing frequency. shRNA-ctr and shRNA-PIP5Kγ–silenced NK92 cells were tested in a ^{51}Cr-release assay toward 721.221-sensitive target cells for 4 hours and 8 hours. Where indicated, the ^{51}Cr-release assay was performed in the presence of cycloheximide. (A) Percentage of specific lysis was used to calculate killing frequency as described in the "Degranulation and cytotoxic assay." Means from 3 independent experiments ± SD are graphed. Differences obtained between shRNA-ctr (gray column) and shRNA-PIP5Kγ (black column) populations at the indicated E:T ratio in the presence of cycloheximide were significant (*$P < .05$). (B) Data represent the shRNA-ctr (♦) or shRNA-PIP5Kγ (●) percentage (means ± SD) of specific lysis of 3 independent experiments of a standard ^{51}Cr-release assay. (C) shRNA-ctr and shRNA-PIP5Kγ-silenced primary cultured NK cells or YTS cells were assessed in a ^{51}Cr-release assay toward K562 and 721.221 targets, respectively. Means from 3 independent experiments ± SD are graphed. Differences between sh-RNA-ctr (gray column) and shRNA-PIP5Kγ (black column) were significant (*$P < .05$).

and was determined by dividing the number of killed targets by the number of effector cells. As shown previously, the killing frequency increases from higher to lower E:T ratios,[8] probably because of a greater possibility for an individual NK cell to form contacts with target cells at lower E:T ratios.

Analysis of the killing frequency demonstrated that NK92 cells were capable of serially killing multiple targets: on average, at the lower E:T ratio, 2-3 targets were killed by an effector after 4 or 8 hours, respectively (Figure 6A left and right panels). At such very low E:T ratios, no reduction of killing frequency was observed in PIP5Kγ-silenced cells. At higher E:T ratios, we observed a significant killing defect in PIP5Kγ-silenced cells in a standard ^{51}Cr-release assay (Figure 6B), indicating that the higher target availability could compensate for the killing defect.

The ability to execute multiple killing cycles partially relies on the new synthesis of cytotoxic components to refill the store of cytotoxic proteins. In agreement with a previous study,[17] treatment with cycloheximide, an inhibitor of the de novo protein synthesis, had no effect on killing frequency in the control population. In these conditions, we observed an increased defect of killing frequency in the PIP5Kγ-silenced population that was more evident in the 8-hour assay, approaching half of the lytic event performed (Figure 6A right panel).

We also assessed the impact of PIP5Kγ silencing on the killing frequency of primary cultured and YTS NK cells (Figure 6C), and our data showed that both NK cell populations exhibited a lower killing frequency with respect to NK92 cells. The lack of a PIP5Kγ-dependent PIP2 pool, induces a significant decrease of killing frequency independently from the presence of cycloheximide.

These experiments indicate that the PIP5Kγ-dependent PIP2 pool affects the ability of NK cells to subsequently kill multiple target cells.

Discussion

The ultimate goal of the present study was to characterize molecular events implicated in the regulation of cytolytic machinery component endocytic recycling. Our major findings were: (1) Munc13-4 translocates to the membrane raft after cytolytic machinery activation, (2) Munc13-4 inducibly associates clathrin adaptor AP-2 and undergoes internalization, (3) the PIP5Kγ-dependent PIP2 pool controls Munc13-4 raft compartmentalization and its clathrin/AP-2–dependent endocytic route, and (4) the perturbation of PIP5Kγ-dependent Munc13-4 internalization is associated with an impairment of the serial killing potential.

In agreement with previous observations,[23,24] we show herein that a significant fraction of PIP2 distributes in discrete microdomains at the plasma membrane, colocalizing with lipid rafts, for which aggregation at the cytolytic synapse has been shown to be instrumental to cytolytic machinery activation.[3,22] We also showed that raft disruption leads to a profound impairment of lytic granule exocytosis induced by a sensitive target contact. Somewhat unexpected was the finding that the lack of raft integrity did not perturb the ability of lytic granules to polarize toward the target contact area, which is known to require PI3K-dependent signals.[25,26] Such a result is in agreement with the observation that the activation of PI3K downstream of the β2 integrin receptor in NK cells was insensitive to cholesterol depletion.[27] In addition, the PI3K p110d isoform, the activation of which is independent of raft-associated src kinase, may also be implicated in the control of granule polarization.[28]

PIP5Ks are essential generators of PIP2. We reported previously that the ubiquitous PIP5Kα and the neuronal PIP5Kγ isoforms represent the major PIP2-synthesizing enzymes in NK

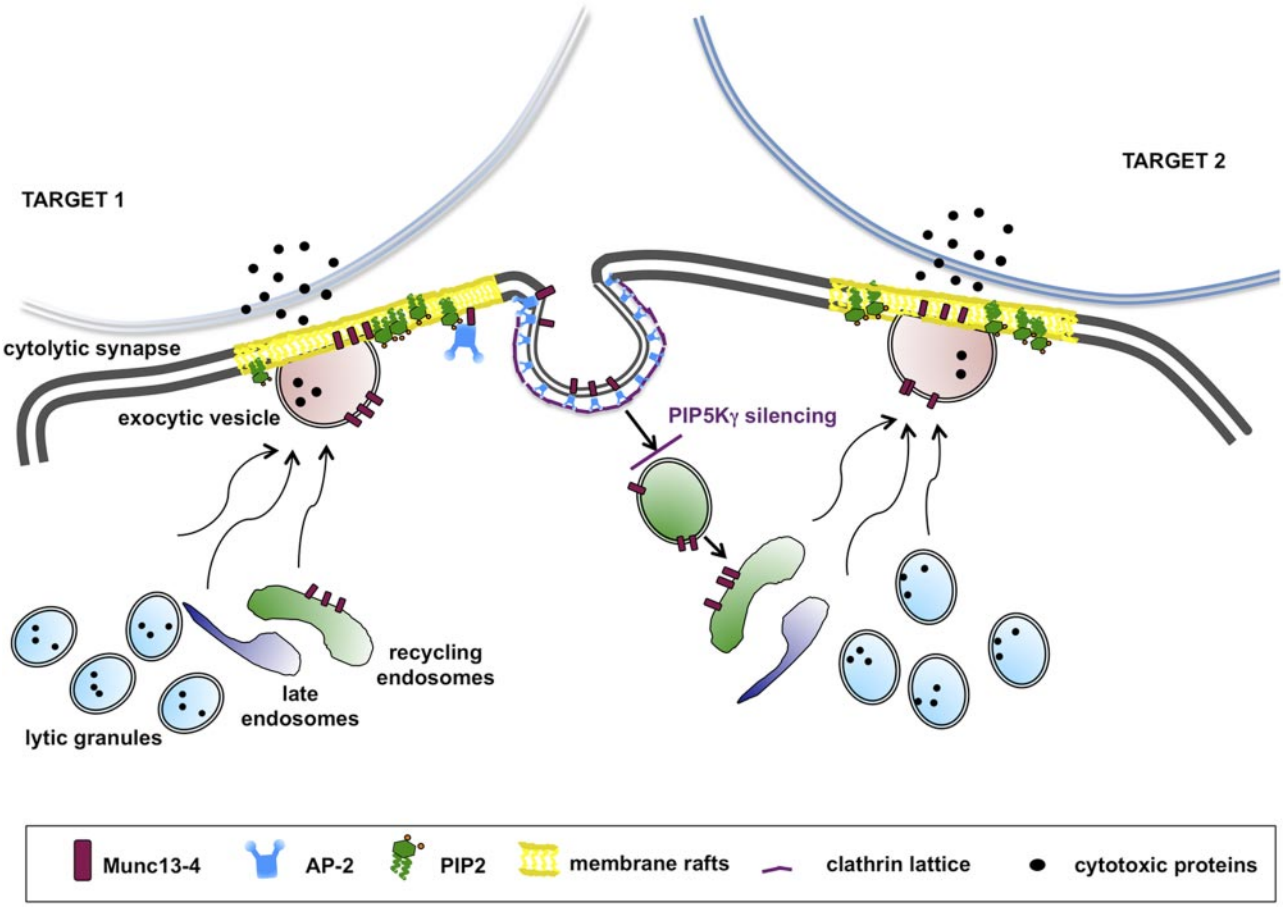

Figure 7. Munc13-4 endocytic recycling is required for the serial killing ability of NK cells. The serial killing model implies that one cytolytic effector can subsequently kill multiple target cells. After target recognition, NK cells form a cytolytic synapse with target cell, where cytolytic granule contents are released. During the cytolytic event, Munc13-4 drives the coalescence of late and recycling endosomes with lytic granule to form the "exocytic vesicles," which fuse with the plasma membrane. Munc13-4 becomes transiently associated with membrane raft microdomains, followed by its subsequent clathrin/AP2-dependent reinternalization. Our model suggests that Munc13-4 retrieval is required for the replenishment of a pool of endocytic vesicles, allowing the subsequent killing event. Our data indicate that the lack of the PIP5Kγ-dependent PIP2 pool leads to impaired clathrin/AP2–mediated retrieval of endocytic machinery components, thus affecting the ability to kill in an iterative manner.

cells.[13] Emerging evidence supports the concept that individual PIP5K isoforms fulfill distinct functions related to their ability to provide spatially and functionally distinct PIP2 pools.[29] By shRNA-driven silencing of individual PIP5K isoforms, we obtained a comparable reduction of PIP5Kα and PIP5Kγ protein levels. Because PIP2 is the phospholipase C substrate, we demonstrated previously that PIP5Kα and PIP5Kγ synergistically control the IP3/Ca^{2+} levels required for granule exocytosis.[13] In the present study, we show that in the absence of the PIP5Kγ-dependent, but not the PIP5Kα-dependent, PIP2 pool, a significant defect of lytic granule secretion occurs despite the presence of Ca^{2+} ionophore, indicating that PIP5Kγ is involved in the control of additional Ca^{2+}-independent events.

Among the SNARE system proteins, Munc13-4 and syntaxin11, defects of which are responsible for FHL type 3 and type 4, play a well-established role in the coordination of activation-induced priming and fusion step of lytic granules, respectively.[5,6,30] The concentration of SNARE factors in membrane rafts and the formation of PIP2/SNARE clusters are believed to be of functional importance in organizing the secretory pathway in neuroendocrine and hematopoietic systems,[31-33] perhaps by defining docking and fusion sites for exocytosis.[34,35]

Analysis of SNARE protein raft compartmentalization showed that Munc13-4 was largely represented in the detergent-soluble fractions of unstimulated cells undergoing raft recruitment after triggering of granule exocytosis by PMA/ionomycin treatment or CD16 engagement. Among the receptors involved in natural killing, DNAM-1 had the unique ability to promote Munc13-4 raft recruitment. The special character of DNAM-1 likely related to its functional association with LFA-1,[36] leading to the hypothesis that LFA-1 couples DNAM-1 to PIP5Kγ[37] in the regulation of Munc13-4. Further, in agreement with a previous study showing that 2B4 and NKG2D stimulation fails to promote Munc13-4 recruitment to perforin-containing granules,[38] we observed that 2B4 or NKG2D individual engagement is not sufficient to induce Munc13-4 raft recruitment. However, the synergistic integration of signals generated from the simultaneous engagement of 2B4 with DNAM-1 or NKG2D leads to Munc13-4 mobilization.

Munc13-4 cellular compartmentalization has been well elucidated in cytolytic effectors. The punctate pattern that we observed in unstimulated cells is in agreement with the well-documented Munc13-4 distribution I the $Rab11^+$ endosomal recycling compartment. After target cell recognition, Munc13-4 allows granule maturation, promoting the coalescence of the recycling vesicle pool with perforin-containing granules, leading to the formation of a unique "exocytic vesicle."[7] At a later step, depending on its interaction with Rab27a, Munc13-4 also exerts a "priming" function, likely by regulating the interaction between vesicle and target SNARE required for granule fusion with the plasma membrane.

The presence of raft-associated Munc13-4 on activation may indicate that the fusion of exocytic vesicle with plasma membrane occurred. Furthermore, constitutive exocytosis through recycling endosomes may also promote Munc13-4 raft recruitment under basal conditions.[4]

The internalization of raft-associated proteins via the clathrin/AP-2–mediated pathway has been widely reported.[39,40] Herein we report that raft-associated Munc13-4 undergoes internalization through a clathrin-dependent route. PIP2 is a key regulator of nearly all stages of clathrin-mediated endocytosis[11]; in particular, PIP5Kγ has been shown to interact with membrane AP-2, providing a local PIP2 pool that allows the recruitment of additional AP-2 complex to the neuronal plasma membrane to trigger clathrin-mediated retrieval of synaptic vesicles.[41-43] Based on the observation that in the absence of the PIP5Kγ-dependent PIP2 pool, Munc13-4 was constitutively present and retained in membrane rafts until the later time points of receptor stimulation, we investigated whether the PIP5Kγ-dependent PIP2 pool controls Munc13-4 reinternalization.

We observed that the Munc13-4/AP-2 interaction is transiently up-regulated on stimulation, indicating that Munc13-4 may represent a cargo for AP-2–dependent endocytic recycling. Indeed, Munc13-4 presents several Yxxϕ and (DE)xxx(LL) motifs that may direct its incorporation into clathrin-coated vesicles via direct AP-2 binding. In the absence of PIP5Kγ, we observed a shift of AP-2 from the membrane, where it becomes active and mediates cargo binding, to the cytosolic compartment,indicating that PIP5Kγ acts in the control of AP-2 membrane compartmentalization.

Our findings lead to the hypothesis that the PIP5Kγ-dependent PIP2 pool is involved in the control of Munc13-4 reinternalization at the cytolytic synapse, allowing its recycling to the steady-state location.

An additional possible mechanism implicating PIP2 in the control of Munc13-4 trafficking is the regulation of the fission factor dynamin, the activity of which requires PIP2 binding via the PH domain.[44] Intriguingly, a role for dynamin2 in the regulation of granule exocytosis has been reported in human NK cells.[45]

Cytolytic effectors are able to execute multiple killing cycles in a short time period.[8,9] The iterative killing ability depends on the combination of 2 factors: (1) that, after target recognition, receptor triggering leads to the release of a fraction of granules; and (2) at the same time, cytotoxic proteins are newly synthesized to refill the store of cytolytic components. Whether secretory lysosome retrieval may also contribute to guaranteeing the serial killing potential is presently unknown.

We hypothesize that Munc13-4 replenishment in the recycling compartment is required to confer iterative cytotoxic activity to the cytolytic effectors. Accordingly, a bidirectional trafficking of lytic granule protein CD107a and immune receptors has been demonstrated at the immune synapse,[10,46] facilitating the recycling and reuse of cytolytic machinery components by cytotoxic cells.

In the present study, we show that in the absence of the PIP5Kγ-dependent PIP2 pool in NK cells, the ability to kill multiple targets by individual effectors is significantly reduced. Our results support the vision that in cell populations with high serial killing potential, such as IL-2–dependent NK92 cells, blocking perforin neosynthesis is required to reveal the impact of PIP5Kγ silencing on killing frequency. Conversely, in NK-cell populations with lower serial killing potential, such as primary cultured and YTS NK cells, recycling of cytolytic machinery components represents a rate-limiting step. In this context, the defect of cytotoxic function observed in FHL patients would also hide a deficiency of serial killing potential.

The tight coupling of endocytic activity to the exocytic pathway is reminiscent of neurologic synapse. Indeed, many effectors of the machinery for docking, priming, and fusion at the cytolytic synapse play a role that is consistent with their roles at the neurologic synapse.[47] This analogy is strengthened by the knowledge that the PIP5Kγ-dependent PIP2 pool regulates clathrin-mediated synaptic vesicle retrieval in humans[48] and in mice.[49] We propose a model applicable to all receptors in which stimulation alone or in combination is able to trigger granule exocytosis: in the absence of PIP5Kγ, initial granule release would occur, but the subsequent burst of granule release would be limited because of the lack of Munc13-4 recycling (Figure 7).

Acknowledgments

The authors thank Dr L. Lenti (Department of Experimental Medicine, Sapienza University, Rome, Italy) for TLC analysis; Dr P. De Camilli for anti-PI5KIγ mAb; Drs H. Horiuchi and S. D. Catz for anti-Munc13-4 Ab; and Dr R. Prekeris for anti-syntaxin11 Ab.

This work was supported by grants from the Italian Association for Cancer Research (AIRC), the Italian Ministry for University and Research (MIUR), and the Center of Excellence (BEMM).

Authorship

Contribution: C.C. performed the experiments, analyzed the data, and helped write the manuscript; R.P. and R.M. performed, acquired, and analyzed the fluorescence-based experiments; L.F. supervised the laboratory activities; A.S. contributed to the research design and discussions on data; and R.G. designed the research, analyzed and interpreted the data, and wrote the manuscript.

Conflict-of-interest disclosure: The authors declare no competing financial interests.

Correspondence: Ricciarda Galandrini, MD, PhD, Department of Experimental Medicine, Sapienza University, Viale Regina Elena 324, 00161 Rome, Italy; e-mail: ricciarda.galandrini@uniroma1.it.

References

1. Orange JS. Formation and function of the lytic NK-cell immunological synapse. *Nat Rev Immunol.* 2008;8(9):713-725.
2. Stinchcombe JC, Griffiths GM. Secretory mechanisms in cell-mediated cytotoxicity. *Annu Rev Cell Dev Biol.* 2007;23:495-517.
3. Lou Z, Jevremovic D, Billadeau DD, Leibson PJ. A balance between positive and negative signals in cytotoxic lymphocytes regulates the polarization of lipid rafts during the development of cell-mediated killing. *J Exp Med.* 2000;191(2):347-354.
4. Stow JL, Manderson AP, Murray RZ. SNAREing immunity: the role of SNAREs in the immune system. *Nat Rev Immunol.* 2006;6(12):919-929.
5. Pachlopnik Schmid J, Cote M, Menager MM, et al. Inherited defects in lymphocyte cytotoxic activity. *Immunol Rev.* 2010;235(1):10-23.
6. Feldmann J, Callebaut I, Raposo G, et al. Munc13-4 is essential for cytolytic granules fusion and is mutated in a form of familial hemophagocytic lymphohistiocytosis (FHL3). *Cell.* 2003;115(4):461-473.
7. Ménager MM, Menasche G, Romao M, et al. Secretory cytotoxic granule maturation and exocytosis require the effector protein hMunc13-4. *Nat Immunol.* 2007;8(3):257-267.
8. Bhat R, Watzl C. Serial killing of tumor cells by human natural killer cells-enhancement by therapeutic antibodies. *PLoS One.* 2007;2(3):e326.
9. Ullberg M, Jondal M. Recycling and target binding capacity of human natural killer cells. *J Exp Med.* 1981;153(3):615-628.
10. Liu D, Bryceson YT, Meckel T, Vasiliver-Shamis G,

Dustin ML, Long EO. Integrin-dependent organization and bidirectional vesicular traffic at cytotoxic immune synapses. *Immunity.* 2009;31(1):99-109.

11. Martin TF. PI(4,5)P(2) regulation of surface membrane traffic. *Curr Opin Cell Biol.* 2001;13(4):493-499.
12. Di Paolo G, De Camilli P. Phosphoinositides in cell regulation and membrane dynamics. *Nature.* 2006;443(7112):651-657.
13. Micucci F, Capuano C, Marchetti E, et al. PI5KI-dependent signals are critical regulators of the cytolytic secretory pathway. *Blood.* 2008;111(8):4165-4172.
14. Galandrini R, Tassi I, Mattia G, et al. SH2-containing inositol phosphatase (SHIP-1) transiently translocates to raft domains and modulates CD16-mediated cytotoxicity in human NK cells. *Blood.* 2002;100(13):4581-4589.
15. Micucci F, Zingoni A, Piccoli M, Frati L, Santoni A, Galandrini R. High-efficient lentiviral vector-mediated gene transfer into primary human NK cells. *Exp Hematol.* 2006;34(10):1344-1352.
16. Molfetta R, Gasparrini F, Peruzzi G, et al. Lipid raft-dependent FcepsilonRI ubiquitination regulates receptor endocytosis through the action of ubiquitin binding adaptors. *PLoS One.* 2009;4(5):e5604.
17. Bryceson YT, March ME, Barber DF, Ljunggren HG, Long EO. Cytolytic granule polarization and degranulation controlled by different receptors in resting NK cells. *J Exp Med.* 2005;202(7):1001-1012.
18. Galandrini R, Micucci F, Tassi I, et al. Arf6: a new player in FcgammaRIIIA lymphocyte-mediated cytotoxicity. *Blood.* 2005;106(2):577-583.
19. Stauffer TP, Ahn S, Meyer T. Receptor-induced transient reduction in plasma membrane PtdIns(4,5)P2 concentration monitored in living cells. *Curr Biol.* 1998;8(6):343-346.
20. Larkin JM, Brown MS, Goldstein JL, Anderson RG. Depletion of intracellular potassium arrests coated pit formation and receptor-mediated endocytosis in fibroblasts. *Cell.* 1983;33(1):273-285.
21. Macia E, Ehrlich M, Massol R, Boucrot E, Brunner C, Kirchhausen T. Dynasore, a cell-permeable inhibitor of dynamin. *Dev Cell.* 2006;10(6):839-850.
22. Fassett MS, Davis DM, Valter MM, Cohen GB, Strominger JL. Signaling at the inhibitory natural killer cell immune synapse regulates lipid raft polarization but not class I MHC clustering. *Proc Natl Acad Sci U S A.* 2001;98(25):14547-14552.
23. Pike LJ, Casey L. Localization and turnover of phosphatidylinositol 4,5-bisphosphate in caveolin-enriched membrane domains. *J Biol Chem.* 1996;271(43):26453-26456.
24. Johnson CM, Chichili GR, Rodgers W. Compartmentalization of phosphatidylinositol 4,5-bisphosphate signaling evidenced using targeted phosphatases. *J Biol Chem.* 2008;283(44):29920-29928.
25. Jiang K, Zhong B, Gilvary DL, et al. Pivotal role of phosphoinositide-3 kinase in regulation of cytotoxicity in natural killer cells. *Nat Immunol.* 2000;1(5):419-425.
26. Tassi I, Klesney-Tait J, Colonna M. Dissecting natural killer cell activation pathways through analysis of genetic mutations in human and mouse. *Immunol Rev.* 2006;214(1):92-105.
27. Riteau B, Barber DF, Long EO. Vav1 phosphorylation is induced by beta2 integrin engagement on natural killer cells upstream of actin cytoskeleton and lipid raft reorganization. *J Exp Med.* 2003;198(3):469-474.
28. Kim N, Saudemont A, Webb L, et al. The p110delta catalytic isoform of PI3K is a key player in NK-cell development and cytokine secretion. *Blood.* 2007;110(9):3202-3208.
29. van den Bout I, Divecha N. PIP5K-driven PtdIns(4,5)P2 synthesis: regulation and cellular functions. *J Cell Sci.* 2009;122(pt 21):3837-3850.
30. zur Stadt U, Schmidt S, Kasper B, et al. Linkage of familial hemophagocytic lymphohistiocytosis (FHL) type-4 to chromosome 6q24 and identification of mutations in syntaxin 11. *Hum Mol Genet.* 2005;14(6):827-834.
31. Kay JG, Murray RZ, Pagan JK, Stow JL. Cytokine secretion via cholesterol-rich lipid raft-associated SNAREs at the phagocytic cup. *J Biol Chem.* 2006;281(17):11949-11954.
32. Chamberlain LH, Burgoyne RD, Gould GW. SNARE proteins are highly enriched in lipid rafts in PC12 cells: implications for the spatial control of exocytosis. *Proc Natl Acad Sci U S A.* 2001;98(10):5619-5624.
33. Salaün C, James DJ, Chamberlain LH. Lipid rafts and the regulation of exocytosis. *Traffic.* 2004;5(4):255-264.
34. Lang T, Bruns D, Wenzel D, et al. SNAREs are concentrated in cholesterol-dependent clusters that define docking and fusion sites for exocytosis. *EMBO J.* 2001;20(9):2202-2213.
35. Aoyagi K, Sugaya T, Umeda M, Yamamoto S, Terakawa S, Takahashi M. The activation of exocytotic sites by the formation of phosphatidylinositol 4,5-bisphosphate microdomains at syntaxin clusters. *J Biol Chem.* 2005;280(17):17346-17352.
36. Shibuya K, Lanier LL, Phillips JH, et al. Physical and functional association of LFA-1 with DNAM-1 adhesion molecule. *Immunity.* 1999;11(5):615-623.
37. Mace EM, Zhang J, Siminovitch KA, Takei F. Elucidation of the integrin LFA-1-mediated signalling pathway of actin polarization in natural killer cells. *Blood.* 2010;116(8):1272-1279.
38. Wood SM, Meeths M, Chiang SC, et al. Different NK cell-activating receptors preferentially recruit Rab27a or Munc13-4 to perforin-containing granules for cytotoxicity. *Blood.* 2009;114(19):4117-4127.
39. Rollason R, Korolchuk V, Hamilton C, Schu P, Banting G. Clathrin-mediated endocytosis of a lipid-raft-associated protein is mediated through a dual tyrosine motif. *J Cell Sci.* 2007;120(pt 21):3850-3858.
40. Deinhardt K, Berninghausen O, Willison HJ, Hopkins CR, Schiavo G. Tetanus toxin is internalized by a sequential clathrin-dependent mechanism initiated within lipid microdomains and independent of epsin1. *J Cell Biol.* 2006;174(3):459-471.
41. Höning S, Ricotta D, Krauss M, et al. Phosphatidylinositol-(4,5)-bisphosphate regulates sorting signal recognition by the clathrin-associated adaptor complex AP2. *Mol Cell.* 2005;18(5):519-531.
42. Nakano-Kobayashi A, Yamazaki M, Unoki T, et al. Role of activation of PIP5Kgamma661 by AP-2 complex in synaptic vesicle endocytosis. *EMBO J.* 2007;26(4):1105-1116.
43. Bairstow SF, Ling K, Su X, Firestone AJ, Carbonara C, Anderson RA. Type Igamma661 phosphatidylinositol phosphate kinase directly interacts with AP2 and regulates endocytosis. *J Biol Chem.* 2006;281(29):20632-20642.
44. Bethoney KA, King MC, Hinshaw JE, Ostap EM, Lemmon MA. A possible effector role for the pleckstrin homology (PH) domain of dynamin. *Proc Natl Acad Sci U S A.* 2009;106(32):13359-13364.
45. Arneson LN, Segovis CM, Gomez TS, et al. Dynamin 2 regulates granule exocytosis during NK cell-mediated cytotoxicity. *J Immunol.* 2008;181(10):6995-7001.
46. Das V, Nal B, Dujeancourt A, et al. Activation-induced polarized recycling targets T cell antigen receptors to the immunological synapse; involvement of SNARE complexes. *Immunity.* 2004;20(5):577-588.
47. de Saint Basile G, Menasche G, Fischer A. Molecular mechanisms of biogenesis and exocytosis of cytotoxic granules. *Nat Rev Immunol.* 2010;10(8):568-579.
48. Narkis G, Ofir R, Landau D, et al. Lethal contractural syndrome type 3 (LCCS3) is caused by a mutation in PIP5K1C, which encodes PIPKI gamma of the phophatidylinsitol pathway. *Am J Hum Genet.* 2007;81(3):530-539.
49. Di Paolo G, Moskowitz HS, Gipson K, et al. Impaired PtdIns(4,5)P2 synthesis in nerve terminals produces defects in synaptic vesicle trafficking. *Nature.* 2004;431(7007):415-422.